

Holography in Porous Silicon

G. Lérondel, S. Setzu, M. Thönissen* and R. Romestain

Laboratoire de Spectrométrie Physique, Université J. Fourier - CNRS (UMR 5588), B.P. 87, 38402 St. Martin d'Heres cedex France

* Institut für Schich- und Ionentechnik (ISI), RFA Jülich, 52425 Jülich Germany

Holographic structures have been obtained in porous silicon (PS) by photodissolution of the material in hydrofluoric acid under interferometric illumination. This process can be performed after or during the formation of the PS layer. One- or two-dimensional structures have been easily etched down to the submicron range. The photosensitivity is demonstrated for the entire visible range. Because the dissolution process occurs in the bulk, the thickness of the structure is only determined by the penetration depth of the light in the material, which in the case of PS is about 0.1 to 15 μm (from uv to 600 nm). The technique is generalized to all types of nanoporous silicon. The efficiency of the dissolution depends on the specific area of the porous material and the initial resistivity of the wafer. The structures have been characterized by light diffraction. For this material, photoluminescence allows the topography of the porosity modulation to be determined precisely. These results and the ease and low-cost fabrication of the PS layer make porous silicon a promising material for holography.

Journal of Imaging Science and Technology 41: 468–473 (1997)

Introduction

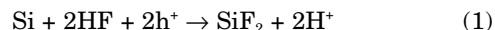
Porous silicon (PS) was discovered in 1956 by Uhlir¹ and Turner² studying the electropolishing of Si substrate in hydrofluoric acid solution. Nevertheless, the largest interest in this material started with the discovery by Canham in 1990 of its photoluminescence at room temperature.³ Since then, this material has given rise to many investigations to explain this property but also to a rediscovery of the potential of this material for optics. The possibility first to make well-defined thin layers and, second, to modulate the refractive index according to the porosity allows PS optical multilayer devices to be made, for example, Bragg reflectors, Fabry-Perot filters,⁴ waveguides,^{5,6} and luminescent microcavities.^{7–9} In all the previous examples, the porosity modulation is obtained by changing the current density of formation and, consequently, in the dissolution direction, i.e., vertical modulation. Some different techniques were used to modulate the porosity in the layer plane, for example, lithography^{10,11} or pulsed laser gratings.¹² Recently, we have shown that a very well-defined PS periodic superstructure can be obtained in the layer plane by photochemical holographic grating.¹³ The photosensitivity was first used to increase the efficiency of the luminescence, because a dissolution and, consequently, an increase of the porosity is observed when a porous silicon layer is in contact with HF under illumination.¹⁴ But holography is well known and used in the industry to produce diffraction gratings.

After a review of the PS formation process, we now present the results of holographic gratings made on porous silicon. Spatially resolved photodissolution is considered for the various types of nanoporous PS. Diffraction and photoluminescence properties are presented. Finally, a quantitative analysis of the grating efficiency is given

by studying the in-situ diffraction during the formation of the structure.

Experimental Details

Basically, the first step of silicon dissolution in hydrofluoric solution involves holes present in the semiconductor²:



In this basic model, the holes come from either the bulk silicon in anodic bias for low and heavily doped p-type (p, p+) and heavily doped n-type (n+) substrates or from electron-hole pairs generated by illumination for low doped n type (n) substrate. The same chemical reaction also occurs without electric bias and has been successfully used in thinning crystallites.¹⁴ If the hole concentration is increased by illumination, the number of dissolved Si atoms unit of time increases consequently. Spatial modulation of the illumination will result in correlated spatial modulation of the porosity. Both techniques have been used: photoformation of porous silicon under electrical bias and photodissolution of an already conventionally formed PS layer. In addition, in comparison with bulk silicon or other semiconductors, the effect of the photochemistry is expected to be enhanced in PS because of the very large specific area of this material, which is one of the main characteristics of the porous medium. The porous silicon layers were obtained by electrochemical dissolution of p- and n-type [100] oriented silicon substrates.

The characteristics, i.e., porosity and dissolution velocity, are controlled by the current density of formation, typically between 5 and 300 mA/cm² and the HF concentration of the electrolyte between 10 and 35% in volume. The formation times vary between several and thousands of seconds for the thickest layers and slowest dissolution velocity. For the illumination, we used both an Ar laser (457 and 515 nm) or a rhodamine 6G dye laser (590 nm). These lines enable the visible range to be covered with sufficient power (on the order of 10 mW/cm²). The size of the laser beam

Original manuscript received March 26th, 1997.

© 1997, IS&T—The Society for Imaging Science and Technology

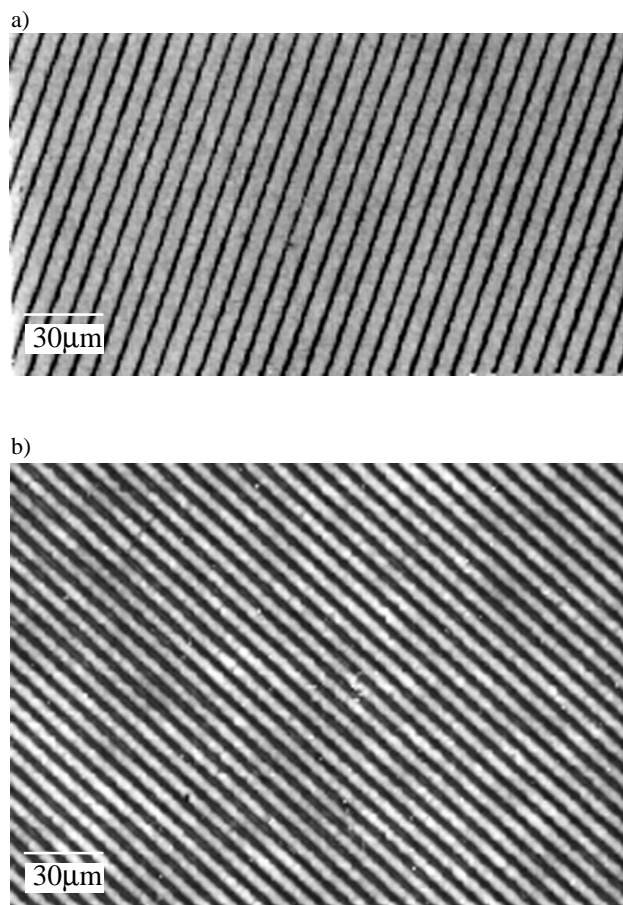


Figure 1. Optical microscope view of PS layers structured using holography and, either the (a) photodissolution or the (b) electrophotodissolution. (a) The PS layer was obtained by electrochemical etching of a low doped p-type Si substrate using a current density of 16.6 mA/cm^2 and a solution of 35% HF concentration. The photodissolution was performed after the PS layer formation in the same solution under green Ar line illumination ($2 \times 10 \text{ mW/cm}^2$) for 15 min. (b) The PS layer was etched under illumination for 120 s in a low doped n-type Si substrate using a current density of 5 mA/cm^2 and an HF concentration of 15%.

was multiplied by 15 using a telescope to illuminate the whole surface of the PS layer (1 cm^2). The interference pattern was obtained after separating the beam using an half beam splitter, which is wedged to remove the spurious interfering beam. Since HF is corrosive for the optics, the formation cell is covered with a CaF_2 window to enable illumination during the photodissolution process. No digital processing was used to improve the photographs shown here.

Results and Discussion

Interferometry and Photodissolution. A clear demonstration of the photosensitivity of PS is given by Fig. 1, which shows an optical microscope view of two porous silicon layers after modulated photodissolution. Figure 1(a) corresponds to a p-type PS layer photodissolved after formation. Figure 1(b) corresponds to a n-type nanoporous Si layer. In this second case, the dissolution was performed during PS formation. In both cases, stripes are clearly visible on the surface, corresponding to a succession of different reflectivity regions. The contrast of these two photos demonstrates the high photosensitivity of the nanoporous silicon for the two main types of substrates. The efficiency of the photodissolution will be discussed later in more detail. A remarkable property of these structures concerns the regularity of the pattern. This is expected for a holographic structure but could be limited by the homogeneity of the photosensitive material. In the case of PS, because very homogeneous porosities are obtained, the limiting factor is given rather by the homogeneity of the illumination. The typical surface area of the modulation for

these samples is about 1 cm^2 . Because the fabrication of a PS layer of 3 and even 4 inches diameter is well controlled, structured surfaces of 45 to 80 cm^2 could be easily obtained. Serious applications of such holographic PS layers as diffractive structures appear realistic.

To investigate the effect of the photodissolution, scanning electron microscopy (SEM) photographs were also performed. Figure 2(a) shows the edge of a p-type sample like Fig. 1(a). The sample was slightly tilted to also see the surface. The porous silicon layer can be divided into two distinct parts. The initial layer thickness is $5 \mu\text{m}$. On the top $2.5 \mu\text{m}$, grooves are clearly visible while the deepest part of the layer remains unchanged. This photograph illustrates that in the case of porous silicon, because the electrolyte can penetrate through the pores, the photodissolution occurs in the volume of the layer, i.e., where electrolyte contact is possible. The limit in depth is given by the penetration of the light in the material. The observed $2.5\text{-}\mu\text{m}$ value is in very good agreement with the penetration depth of the green Ar laser line in a 57% porous layer ($3 \mu\text{m}$). The shape of the profile theoretically results from the combination of the interference modulation and the absorption as shown later by expression 3. Nevertheless for a very high porosity region, it is well known that cracking of the porous medium appears.¹⁵ We have also observed such an effect.

A critical porosity can be defined. Above this limit, PS is totally removed. Figure 2(b) shows a view of the edge of the sample [Fig. 1(b)] (n-type). The effect of the electrophotodissolution also leads to porosity modulation. The sine profile of the illumination with a period of $6 \mu\text{m}$ resulting from the two laser beam interferences

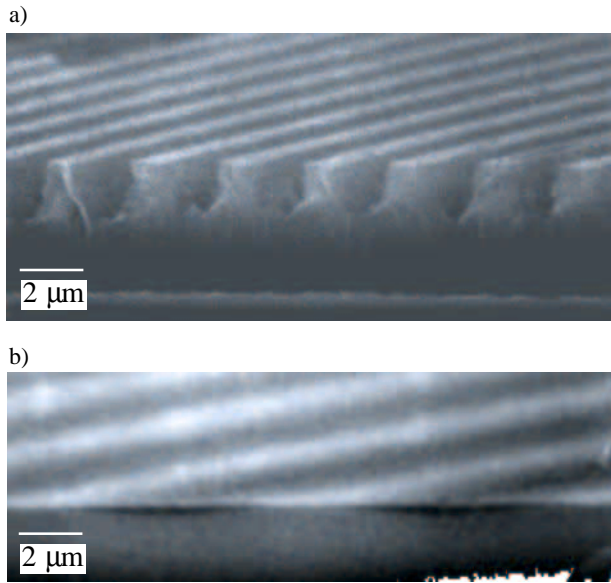


Figure 2. SEM photographs of PS layers. (a) p-type PS layer, with formation and dissolution parameters similar to Fig. 1(a), only the angle of incidence of the two laser beams was increased to obtain smaller periodicity of modulation. (b) see Fig. 1(b). In both cases, the photodissolution takes place in the volume of the porous medium. Depending on the illumination density and photodissolution time porous silicon can be (a) totally removed or (b) partially dissolved. For the n-type, the intrinsic concentration of holes is so low that PS formation occurs only in the illuminated part, i.e., bright fringes.

is reproduced in the limit of the porous medium. The depth of the structure is $0.5 \mu\text{m}$, which corresponds to the PS layer thickness. True electrochemical etching of low doped n-type Si gives rise, after about $1 \mu\text{m}$, to macroporous formation.¹⁶ These SEM photographs show that the photodissolution takes place in volume. Thus, PS enables indepth holography.

Lateral porosity modulation can be observed by spatially resolved luminescence. Figure 3 shows a photograph of the sample [Fig. 2(a)] under UV excitation. Stripes are also clearly visible. The modulated photodissolution leads to an increase of the porosity, so that starting with a nonluminescent PS layer, light emission is only observed from the illuminated part of the sample, which correspond to the bright fringes. The luminescence analysis corroborates the previous observations.

Multistructure and Diffraction Pattern. Usually, to structure the layer plane in more than one direction, many laser beams must be used, i.e., the number of lasers is determined by the desired number of directions. Because the various laser beams, by linear combination, create interferences in undesired directions, they must be coupled 2×2 . However, complicated optical setups are then necessary. More easily here, we have created multistructures by successive photodissolutions. The various directions were simply obtained by rotation of the cell to the desired angles. Figure 4(a) shows an hexagonal array obtained on an n⁺-type PS layer. The periodicity in the three directions is $7.82 \mu\text{m}$. Because the structures are periodic at a micron scale, diffraction patterns are observed on illumination by a laser beam. Figure 4(b) shows the diffraction pattern of the hexagonal structure. The 0th order is surrounded by 6 first orders of diffraction confirming the 6th

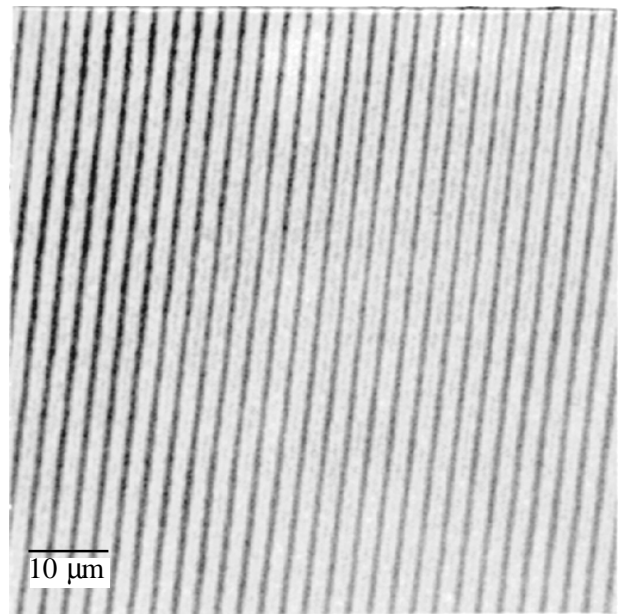


Figure 3. Luminescence photograph of a 1-D PS structured layer. The sample characteristics are given in the Fig. 1 caption. The luminescence is close to the photodissolved part of the sample, corresponding to the bright fringes. The record was done under an optical microscope with a 3200 ISO film.

order symmetry. The large number of multiple orders proves the high diffraction efficiency.

The observed modulation of the intensity in the three directions can be explained by the sample formation. The three gratings were created successively during the formation. Therefore, the sample can be seen as a stack of three lateral porosity modulations. Figure 5(a) shows a decagonal structure made in p-type PS. Slightly below the center, a decagon elementary cell clearly shows the 10th order symmetry. Figure 5(b) shows the diffraction pattern of the decagonal structure previously presented. The 0th order of diffraction is also surrounded by a multitude of secondary orders. The five directions of photodissolution are each characterized by their two first orders of diffraction. They appear as the second most intense points forming a regular decagon. This decagon is itself surrounded by 10 regular pentagons showing the 5th order symmetry.

As regards the intensity, some directions predominate. This is because PS is in a dynamic state during the process. Optical absorption and mechanical stability do not remain unchanged during the different photodissolution steps, so all the directions of photodissolution are not equivalent. Nevertheless, this could be corrected by optimization of the photodissolution parameters and more precisely by in-situ observation of the diffraction intensities in the different directions. Regarding the two diffraction figures, the high spatial selectivity of the etching process in the material and the periodicity obtained by holography give rise to regular arrays of diffraction.

To quantify the diffraction efficiency, we have measured the intensity of diffraction as a function of the order. The spatial periodicity of the structure is derived from the diffraction order position by the following formula:

$$a = \frac{m\lambda}{\sin(\theta_k) - \sin(\theta_i)}, \quad (2)$$

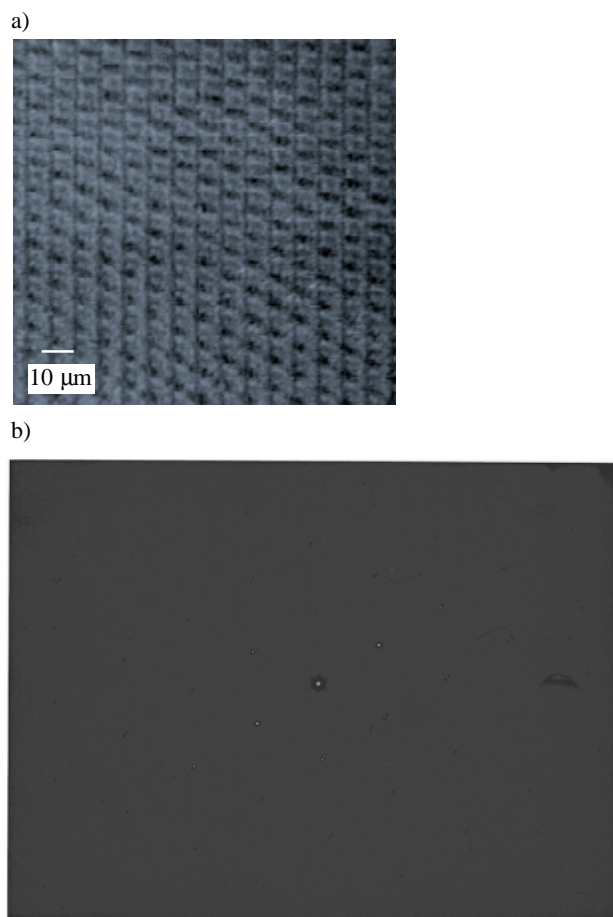


Figure 4. Hexagonal PS multistructure made by holography. (a) optical microscope view of a n^+ type sample obtained after three successive photodissolutions at 120° during the layer formation in HF 10% under 5 mA/cm^2 . The laser wavelength and power were 515 nm and 10 mW/cm^2 , respectively. The elementary hexagonal cell is clearly visible attesting from the 6th-order symmetry. (b) Diffraction pattern of the previous sample. Three directions of photodissolutions are characterized by the hexagonal symmetry of the secondary orders surrounding the specular reflection.

where θ_i is the incident angle of the laser beam, k the order of diffraction, θ_k the angle of the k th order of diffraction, and λ the wavelength of the illumination (HeNe laser line, 632.8 nm). Figure 6(a) shows the diffraction pattern of the n -type 1-D PS holographic structure discussed earlier. We observe here the interesting phenomenon that secondary orders are more intense than specular reflection. This was confirmed by Fig. 6(b) showing the diffraction intensity as a function of the order. This characteristic is well known for mechanical diffraction gratings, which have a so-called *blaze* angle. Here, we propose another interpretation. A view of the structure is given by Fig. 2(b). The diffraction pattern essentially consists of a sine function modulated in the amplitude by the absorption:

$$n(x,z) = n_0 [1 - \alpha I_0 \sin^2(k_x x) \exp(\alpha z)] \quad (3)$$

where n_0 is the initial number of Si atoms (black fringes), α the absorption coefficient, and I_0 the illumination intensity. A complete analysis must take into account the evolution of the material during the photodissolution and the related variation of α . We consider here the photodissolution as a small perturbation. For such a profile, no blaze effect is expected.

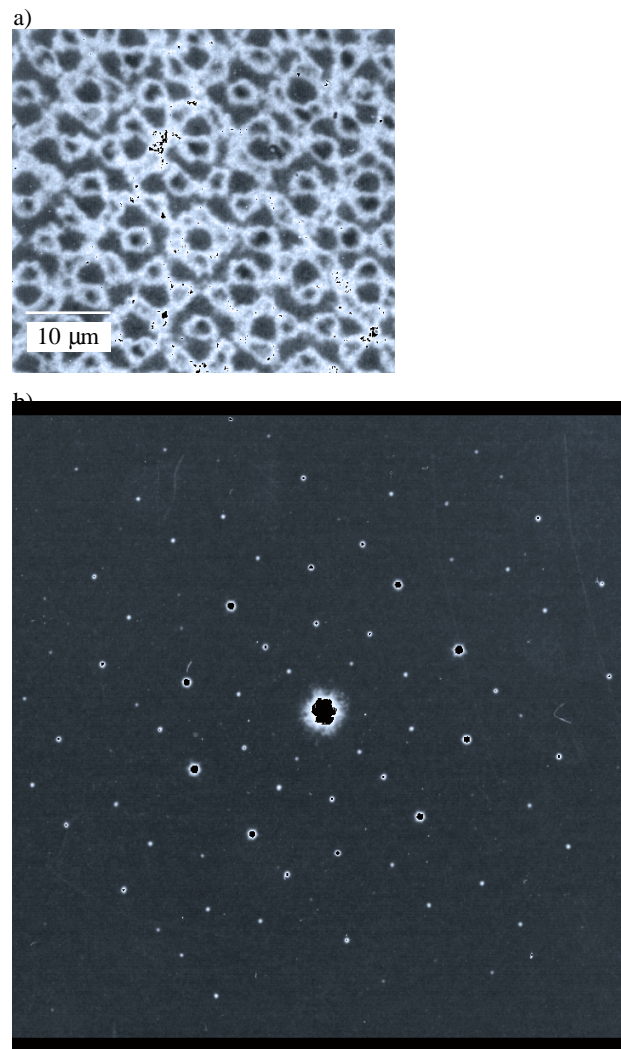


Figure 5. Decagonal PS multistructure made by holography. (a) Optical microscope view of a p -type PS layer after five successive photodissolutions at 72° in a 35% HF solution. Each photodissolution takes 2 min 30 s under 10 mW/cm^2 of illumination (515 nm). The elementary cell at the center of the figure presents a decagonal symmetry as expected. (b) Diffraction pattern of the previous layer. The high regularity and efficiency of the photodissolution lead to a multitude of secondary orders surrounding the specular reflection. Rotation symmetry of the 10th order and a pentagonal pattern are clearly visible.

All of the PS holographic structures that are presented consist of thin layers. They are structured after or during the formation, but in all cases their thicknesses are on the order of 1 to $10 \mu\text{m}$. Because porous silicon is not completely absorbent in the visible range, optical fringes are observed. This means that diffraction intensities are modulated by the thin layer effect. If the specular reflection corresponds to a minimum of the fringes and the angle of diffraction corresponds to a maximum, more intensity is observed in the first-order direction of diffraction than in the specular reflection. Such structures could be used as a light beam separator. The effect of the structured layer thickness on the diffraction intensity is detailed in the following section.

In-Situ Diffraction Analysis. To analyse the effect of localized photodissolution, we performed in-situ measurement of the first-order diffraction intensity. The laser

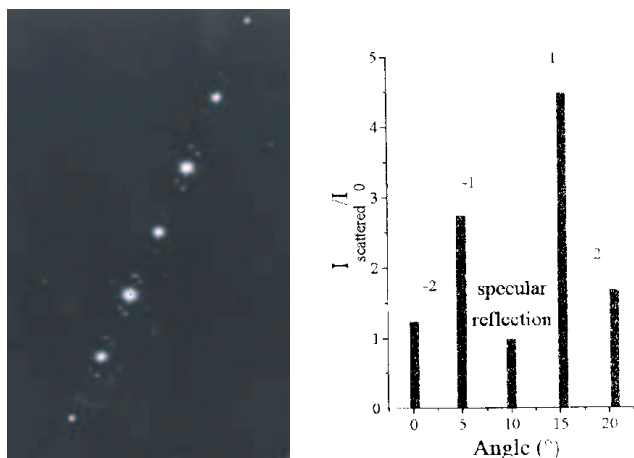


Figure 6. Diffraction study of a thin PS structured layer. The sample characteristics are given in the Fig. 1(b) caption. (a) Diffraction pattern photograph. The 0th order of diffraction is surrounded by the secondary order, and surprisingly, the -1 and 1 orders are more intense than the specular reflection. This was confirmed by the analysis of the diffraction peaks b). The angle of incidence was 10° , and the periodicity derived from the order position was $7.19 \pm 0.11 \mu\text{m}$.

beams used to produce interferences are diffracted by the structure they create. Thus, one can record the intensity of diffraction as a function of time during the photosensitive etching. Figure 7(a) shows a record of the photodissolution of a p-type PS layer previously formed. The intensity of the first order of diffraction (solid points) increases before reaching a maximum and decreases almost to zero for the longest dissolution time. For times between 0 and 200, quadratic dependence is observed (line). The variation of Δn is thus linear with time. Because the number of photodissolved atoms, i.e., porosity, increases linearly with time, the refractive index also depends linearly on the porosity, p :

$$\Delta n(t) \propto p(t) - p_0 \quad (4)$$

where p_0 is the initial porosity of the PS layer or which is equivalent to the porosity at the position of the dark fringes. Such a linear dependence is remarkable, especially considering that for a dry PS layer this dependence is much more complicated.¹⁷ It has already been observed in our group for PS in the HF environment.¹⁸ This behavior, called Clausius-Mosotti law, is common for diluted species in solution. Consequently, for relatively high porosity, i.e., $p_0 = 72\%$, the PS layer filled with the electrolyte can be seen as a dielectric region equivalent to a solution of HF with diluted Si atoms. This simple law enables the effect of the photodissolution and also the efficiency of the diffractive structure to be estimated. For longer times, as shown by Fig. 7, the intensity reaches a maximum before decreasing.

Theoretically, during the photodissolution, the diffracting profile changes from a sine shape to a Dirac function shape. As a consequence, energy transfers from the first-order of diffraction to the secondary order, and then a decrease of the first-order intensity occurs. In fact, exactly at the moment when the maximum is reached, we observed a halo surrounding the spot showing the spurious scattering effect. To explain this, we invoke the mechanical instability of the layer, which gives rise to micrometric cracking. Qualitatively, for the recordings during the formation, similar time dependencies are observed. However, there are some differences.

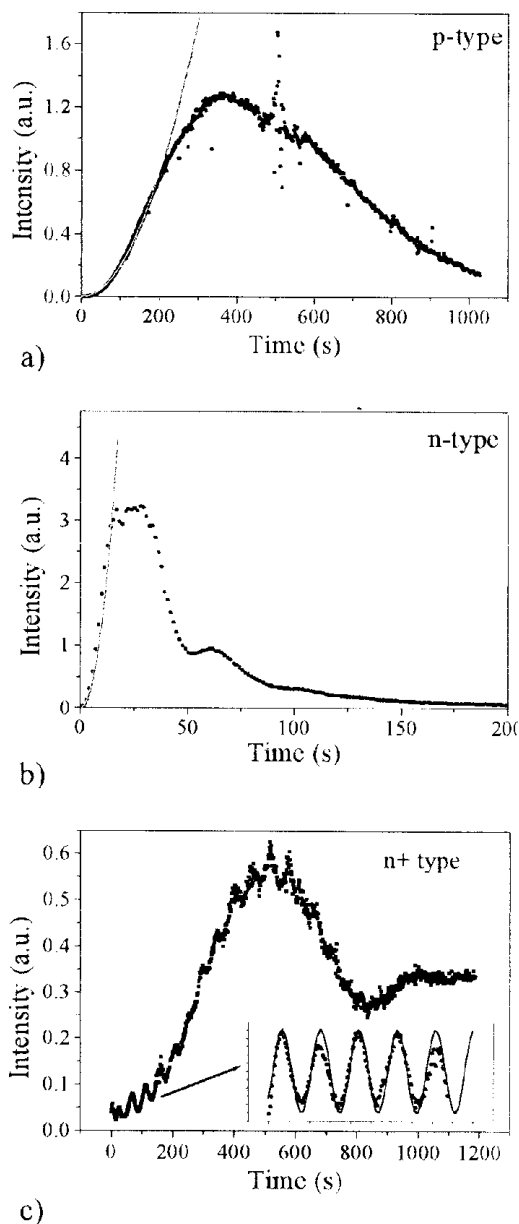


Figure 7. In-situ records of the diffraction intensity. The laser beam used to create interferences is used as a probe beam to observe the PS structure formation. (a) Photodissolution of a p-type PS layer of $4 \mu\text{m}$ thickness and 72% porosity previously etched. (b) Electrophotodissolution of an n-type PS layer [see Fig. 1(b) caption for the conditions]. (c) Electrophotodissolution of a highly doped n-type substrate. The formation parameters were 5 mA/cm^2 for the current density, 10% HF concentration for the electrolyte, and 515 nm for the illumination ($2 \times 10 \text{ mW/cm}^2$). Thickness fringes are clearly visible.

Figure 7(b) shows diffraction intensity as a function of time for the n-type PS layer. Again a quadratic increase of the intensity as a function of time is observed before reaching a maximum and then a decrease. Nevertheless, the increase occurs very fast. The maximum of the efficiency is reached after only 20 s. These three curves can be compared with regards to the amplitude, and we observed that the highest efficiency is obtained for the n-type PS. Due to the depletion of holes in bulk, the effect of the photodissolution is very strong here and the spatial selectivity is

very high [see Fig. 2(b)]. The nonilluminated part remains nonporous, while the porosity of the illuminated part is close to 90%. The refractive index modulation can reach values of about $n_{\text{Si}} - 1 \approx 3$ in the visible range. The right part of the curve can be explained by the formation of n -type nanoporous silicon. The decrease here can be due to scattering, coming from the onset of macropore formation¹⁷ or as for the p -type, from a cracking of the porous region because of the high porosity. The modulations observed in the record are attributed to the optical fringes resulting from the thickness variation. Figure 7(c) is also related to formation but for the n^+ -type substrate. Again an increase and then a decrease are observed, but in addition modulation occurs. Because the photodissolution occurs during the formation, the depth of the diffractive profile is not constant but increases linearly with time. From an optical point of view, fringes appear with a time period of

$$T = \frac{\lambda}{2nv}, \quad (5)$$

where v is the dissolution velocity, n the refractive index of the layer, and λ the illumination wavelength. To illustrate this we performed a simulation of the first five fringes after subtracting the slow parabolic increase [Fig. 7(c) inset]. From this we can derive the periodicity and, knowing the dissolution velocity, the refractive index. A value of 1.7 was obtained, which corresponds to a porous silicon layer of 85% porosity in the HF environment. This shows that the diffraction intensity for the thin layer modulated structure is strongly affected by the optical interferences, as illustrated in Fig. 6(a).

To complete the study, we also created holographic structures in heavily doped p -type PS layers. As expected, because of the important initial concentration of holes in the bulk, the contrast of the photodissolution is much lower than for the three other types of nanoporous silicon. Nevertheless, diffraction effects were observed, showing a porosity modulation. This property is important for the fabrication of lateral photon confinement devices, because p^+ vertical superstructures, such as microcavities, already exist.^{6,7}

Conclusion

PS lateral structures have been obtained by a combination of the photosensitivity of the material and hologra-

phy. Because the high specific area of the porous medium, photodissolution occurs rapidly and is not limited to the surface. In-depth holography is then possible. The quality of the diffraction pattern structure shows the high selectivity and efficiency of the photochemical process. With regards to the periodicity of the structure, whereas values of 0.5 μm have been reached and can probably be optimized, the diffusion of the carriers in the material constitutes a limiting factor. Nevertheless, smaller patterns could be obtained by combination with other techniques well known in PS technology, like thermal oxidation. Interestingly, diffraction properties, which can be the subject of further analysis, are obtained by the combination of lateral and in-depth interferences. In view of these points, porous silicon appears a promising new material for holography. \blacktriangle

References

1. A. Uhlir, *Bell Sys. Tech. J.* **333** (1956).
2. D. R. Turner, *J. Electrochem. Soc.* **105**, 402 (1958).
3. L. T. Canham, *Appl. Phys. Lett.* **57**, 1046 (1990).
4. M. G. Berger, S. Frohnhoff, W. Theiss, U. Rossow, and H. Munder, in *Porous Silicon Science and Technology*, Springer-Verlag, Berlin, 1995, p. 345.
5. A. Loni, L. T. Canham, M. G. Berger, R. Arens-Fischer, H. Munder, H. Luth, H. Arrand, and T. M. Benson, *Thin Solid Films*, **276**, 143 (1996).
6. I. Mihalcescu, G. Lerondel and R. Romestain, *Thin Solid Films*, **297** (1997) 245.
7. V. Pellegrini, A. Tredicucci, C. Mazzoleni and L. Pavesi, *Phys. Rev. B* **52**(20), R14328 (1996).
8. M. Araki, H. Koyama, and N. Koshida, *Jpn. J. Appl. Phys.* **35**, 557 (1996).
9. G. Lerondel, P. Ferrand, and R. Romestain, *MRS Proceeding*, **452**, 631 (1997).
10. A. G. Nassiopoulou, S. Grigopoulos, L. Canham, A. Halimaoui, I. Berbezier, E. Gogolides and D. Papadimitriou, *Thin Solid Films* **255**, 329 (1995).
11. M. Kruger, R. Arens-Fischer, M. Thonissen, H. Munder, M. G. Berger, H. Luth, S. Hilbrich and W. Theiss, *Thin Solid Films* **276**, 257 (1996).
12. A. V. Alexeev-Popov, S. A. Geveliyuk, Ya. O. Roizin, and D. P. Savin, *Solid State Comm.* **97**(7), 591 (1996).
13. G. Lerondel, M. Thonissen, S. Setzu, R. Romestain, and J. C. Vial, *MRS Proceeding*, **452**, 711 (1997).
14. A. Bsiesy, J. C. Vial, F. Gaspard, R. Herino, M. Ligeon, F. Muller, R. Romestain, A. Wasiela and A. Halimaoui and G. Bomchil, *Surf. Sci.* **254**, 195 (1991).
15. O. Belmont, D. Bellet, and Y. Brchet, *J. Appl. Phys.* **79**, 7586 (1996).
16. W. Theiss, S. Henkel, and M. Arntzen, *Thin Solid Films* **255**, 177 (1995).
17. S. Letant and J. C. Vial to be published in *J. Appl. Phys.* **80**(12), 7018 (1996).
18. C. Levy-Clement, in *Porous Silicon Science and Technology*, J. C. Vial and J. Derrien (eds), Springer Verlag, Berlin, 1995, 329.